APPENDICES

APPENDIX A

Coal and Char Characterisation and Results

A-1 Description of Standard Methods Used for Characterisation

ASTM 3682: Standard test method for major and minor elements in combustion residues from coal utilization processes.

CKS 561 (1982): Specification for anthracitic and bituminous coals.

ISO 7404-2 (1994): Methods for the petrographic analysis of bituminous coal and anthracite-Part 2: Preparation of coal samples.

ISO 7404-3 (1994): Methods for the petrographic analysis of bituminous coal and anthracite-Part 3: Method of determining maceral group composition.

ISO 7404-4 (1994): Methods for the petrographic analysis of bituminous coal and anthracite-Part 4: Method of determining microlithotype-, carbominerite- and minerite- composition.

ISO 7404-5 (1994): Methods for the petrographic analysis of bituminous coal and anthracite-Part 5: Method of determining microscopically the reflectance of vitrinite.

ISO 11760 (2005): Classification of coals (ISO, 2009). ISO 12902 : Determination of total carbon, hydrogen and nitrogen-instrumental methods.

ISO 19759: Determination of total sulphur through IR spectroscopy.

SABS ISO 562 (1998): Hard coal and coke: Determination of volatile matter.

SABS 925 (1978): Moisture content of coal samples intended for general analysis: vacuum oven method.

SABS ISO 1171 (1997): Solid mineral fuels: Determination of ash content.

SABS ISO 1928 (1995): Determination of gross calorific value by the bomb calorimetric method, and calculation of net calorific value.

A-2 Vitrinite Reflectance Scan Histograms of Coal Samples

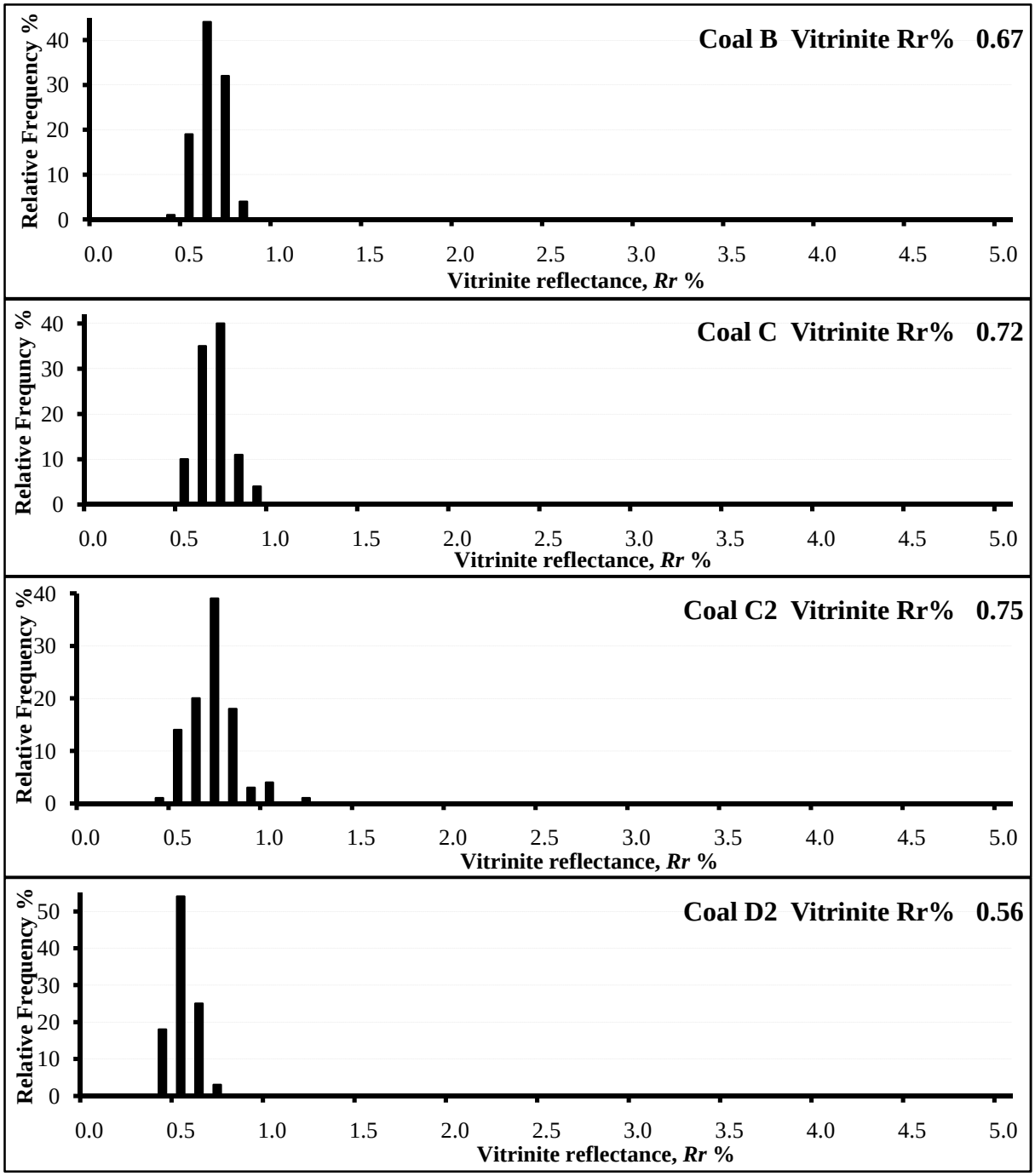

Figure A-1: Vitrinite reflectance scans histogram of the coal samples.

A-3 Total Maceral Reflectance Scan Histograms of Coal and Char samples

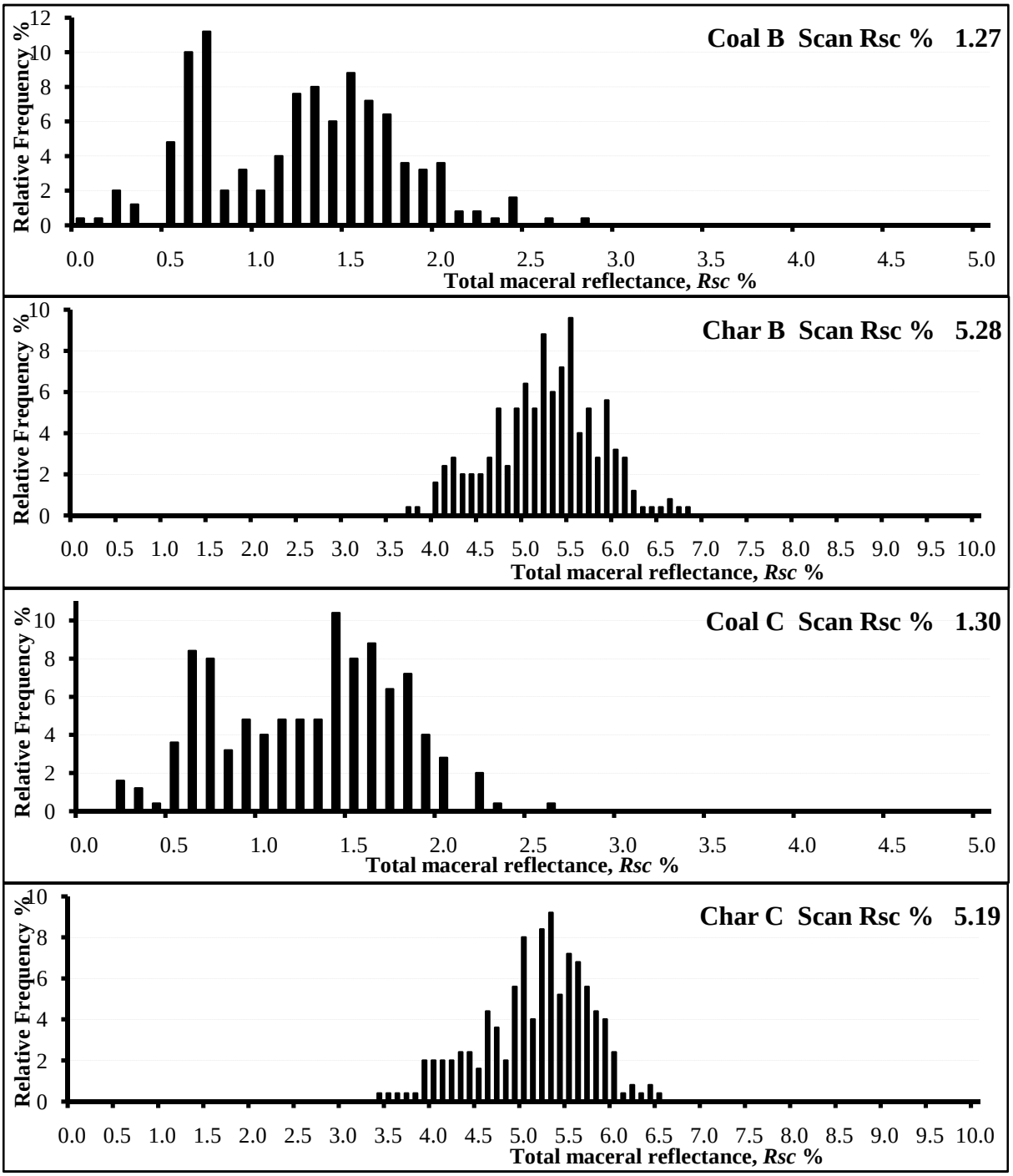

Figure A-2: Total maceral reflectance scans histogram for coals and chars: B and C.

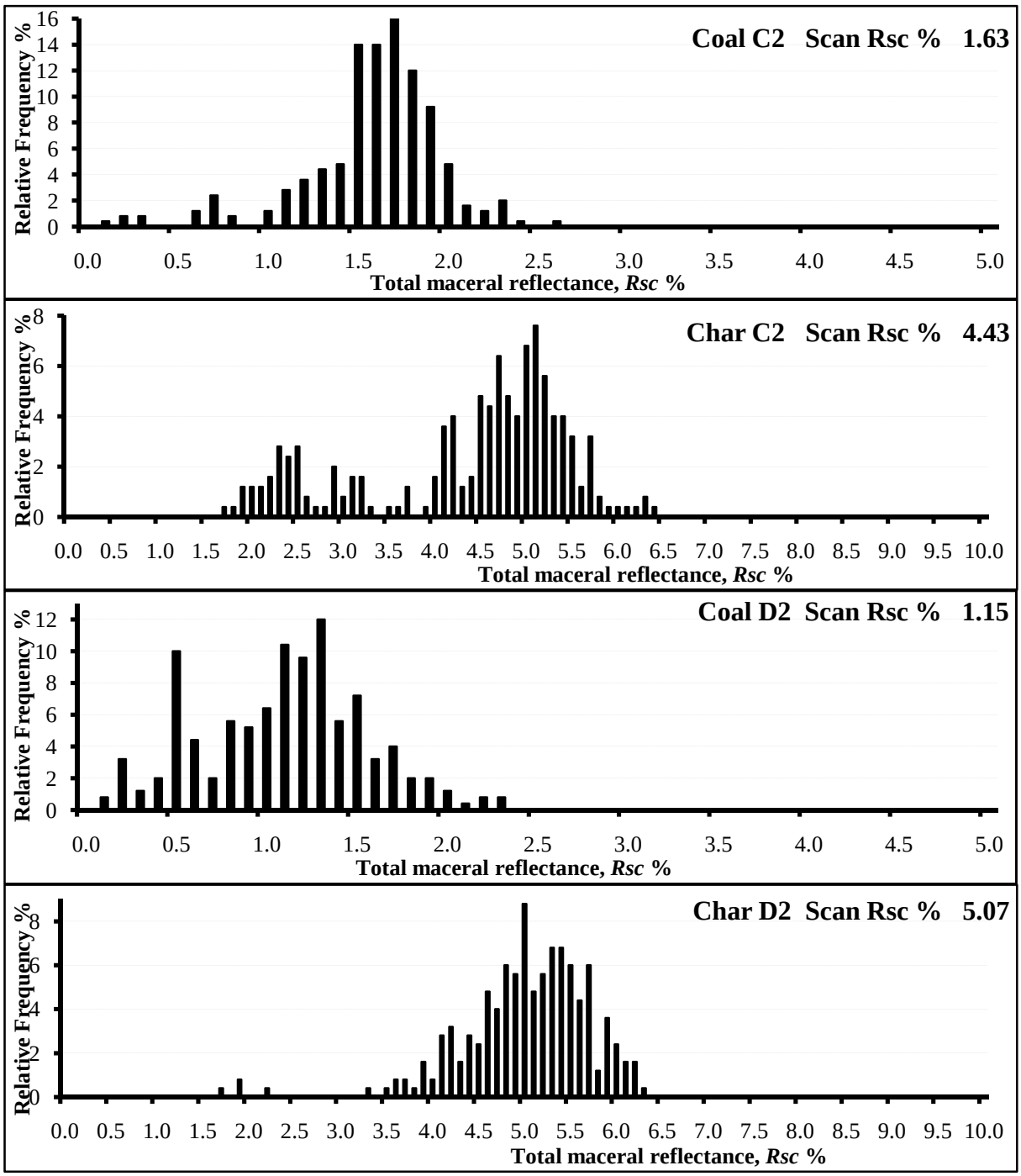

Figure A-3: Total maceral reflectance scans histogram for coals and chars: C2 and D2.

A-4 Outline of Classification System for Char Carbon Forms (du Cann, 2008).

Group A Char carbon forms

Category A1(i): Dense char with frequent tiny pores from vitrinite.

Category A1(ii): Dense char with frequent tiny pores from inertinites.

Category A2: Char networks: fine walled more open networks from coal reactives.

Category A3: Char networks: thicker walled networks form inerts.

Group B Char carbon forms

Category B4: "Coke"- circular anisotropic - fine.

Category B5: "Coke"- circular anisotropic - medium.

Category B6: "Coke"- incipient anisotropic.

Category B7: Thick walled "coke"- isotropic (from coal vitrinite).

Group C Char carbon forms

Category C8: "Oxidised"- mainly from vitrinite.

Category C9: "Oxidised"- mainly from inertinite.

Category C10: "Oxidised"- Low reflecting network.

Group D Char carbon forms

Category D11(i): Original coal - unaffected from vitrinite

Category D11(i): Original coal - unaffected from inertinite

Category D12: Original coal - partially reacted macerals

Group E Char carbon forms

Category E13: Inorganic matter derived from minerals in the original coal

Category E14: Inorganic matter derived from other sources related to the parent coal

Category E15: Process derived depositional carbons (pyrolytic and spherulitic carbons)

APPENDIX B

Char-CO_2 Gasification Reactivity Results

B-1 Reproducibility of Experimental Results and Reactivity of the Chars

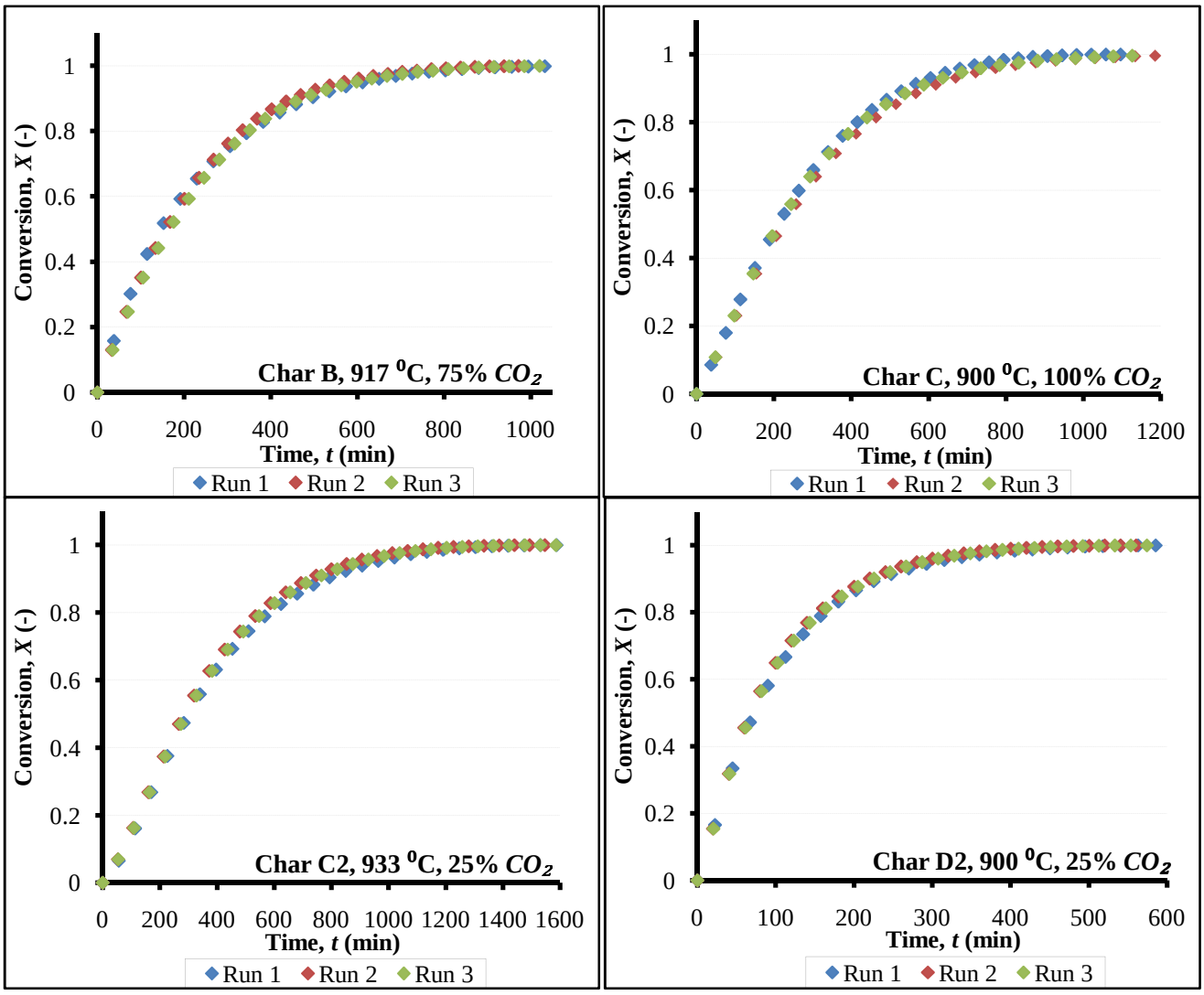

Figure B-1: Reproducibility results for chars B, C, C2 and D2 at different experimental conditions, 0.875 *bar*.

Table B-1: Analysis of reproducibility and experimental error.

	Run 1	Run 2	Run 3	Ave.	σ	Ave. Dev	% Ave. Dev
Char B, 917 ℃, 75% CO_2							
$R \cdot 10^{-2}\ (min^{-1})$	3.070	3.060	3.110	3.08	$2.47 \cdot 10^{-5}$	$1.88 \cdot 10^{-5}$	0.609
$t_f \cdot 10^{-2}\ (min^{-1})$	2.870	2.720	2.760	2.78	$7.78 \cdot 10^{-5}$	$5.78 \cdot 10^{-5}$	2.070
ψ (-)	1.1696	1.1595	1.1768	1.1686	0.0087	0.0061	0.520
$t_{0.5}\ (min)$	162.97	158.10	160.47	160.51	2.430	1.640	1.020
$t_{0.9}\ (min)$	549.93	545.65	553.83	549.80	4.090	2.770	0.500
Char C, 900 ℃, 100% CO_2							
$R \cdot 10^{-2}\ (min^{-1})$	2.370	2.290	2.260	2.310	$5.73 \cdot 10^{-5}$	$4.21 \cdot 10^{-5}$	1.820
$t_f \cdot 10^{-2}\ (min^{-1})$	2.490	2.490	2.460	2.480	$2.07 \cdot 10^{-5}$	$1.59 \cdot 10^{-5}$	0.640
ψ (-)	2.1216	2.2469	2.2029	2.1870	0.060	0.044	1.990
$t_{0.5}\ (min)$	211.20	218.75	215.47	215.14	3.790	2.630	1.220
$t_{0.9}\ (min)$	543.13	555.43	547.10	548.56	6.280	4.590	0.840
Char C2, 933 ℃, 25% CO_2							
$R \cdot 10^{-3}\ (min^{-1})$	1.670	1.680	1.710	1.680	$2.11 \cdot 10^{-5}$	$1.61 \cdot 10^{-5}$	0.960
$t_f \cdot 10^{-3}\ (min^{-1})$	1.820	1.780	1.810	1.800	$2.25 \cdot 10^{-5}$	$1.72 \cdot 10^{-5}$	0.950
ψ (-)	2.0101	2.191	2.2348	2.1453	0.120	0.090	4.200
$t_{0.5}\ (min)$	300.08	294.77	300.66	298.50	3.250	2.490	0.830
$t_{0.9}\ (min)$	781.03	772.80	788.26	780.70	7.730	5.260	0.670
Char D2, 900 ℃, 25% CO_2							
$R \cdot 10^{-2}\ (min^{-1})$	6.870	6.790	6.900	6.850	$5.30 \cdot 10^{-5}$	$3.95 \cdot 10^{-5}$	0.58
$t_f \cdot 10^{-2}\ (min^{-1})$	6.900	6.810	6.910	6.870	$5.60 \cdot 10^{-5}$	$4.29 \cdot 10^{-5}$	0.62
ψ (-)	1.2117	1.2859	1.3051	1.2676	0.049	0.037	2.940
$t_{0.5}\ (min)$	72.82	70.55	71.61	71.66	1.130	0.770	1.080
$t_{0.9}\ (min)$	232.47	219.17	222.45	224.70	6.930	5.180	2.310

B-2 Determination of CO_2 Reactivity of the Chars

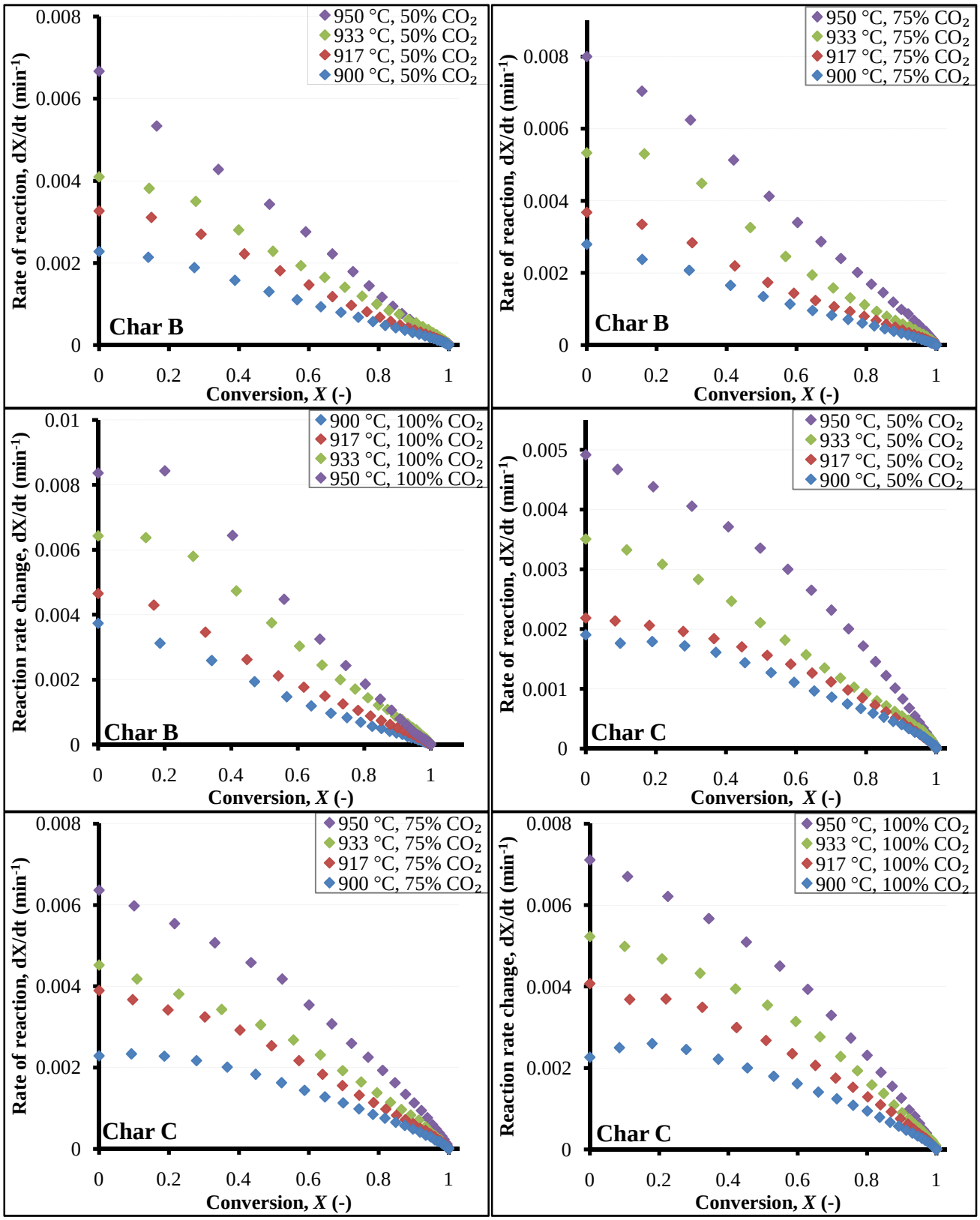

Figure B-2: Rate of reaction versus fractional conversion for chars B and C at different experimental conditions, 0.875 *bar*.

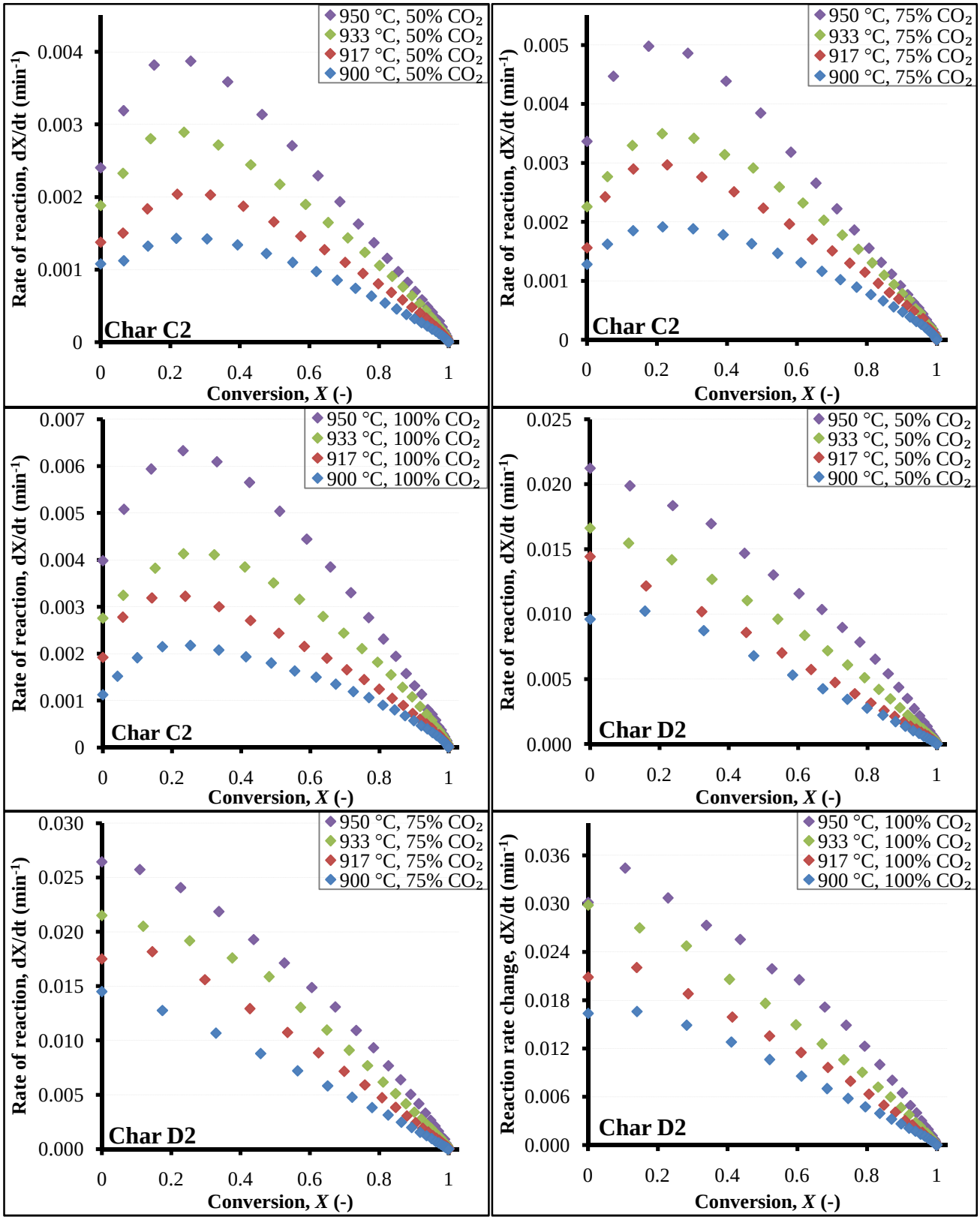

Figure B-3: Rate of reaction versus fractional conversion for chars C2 and D2 at different experimental conditions, 0.875 *bar*.

B-3 Effect of Isothermal Temperature of Reaction on the Char Reactivity

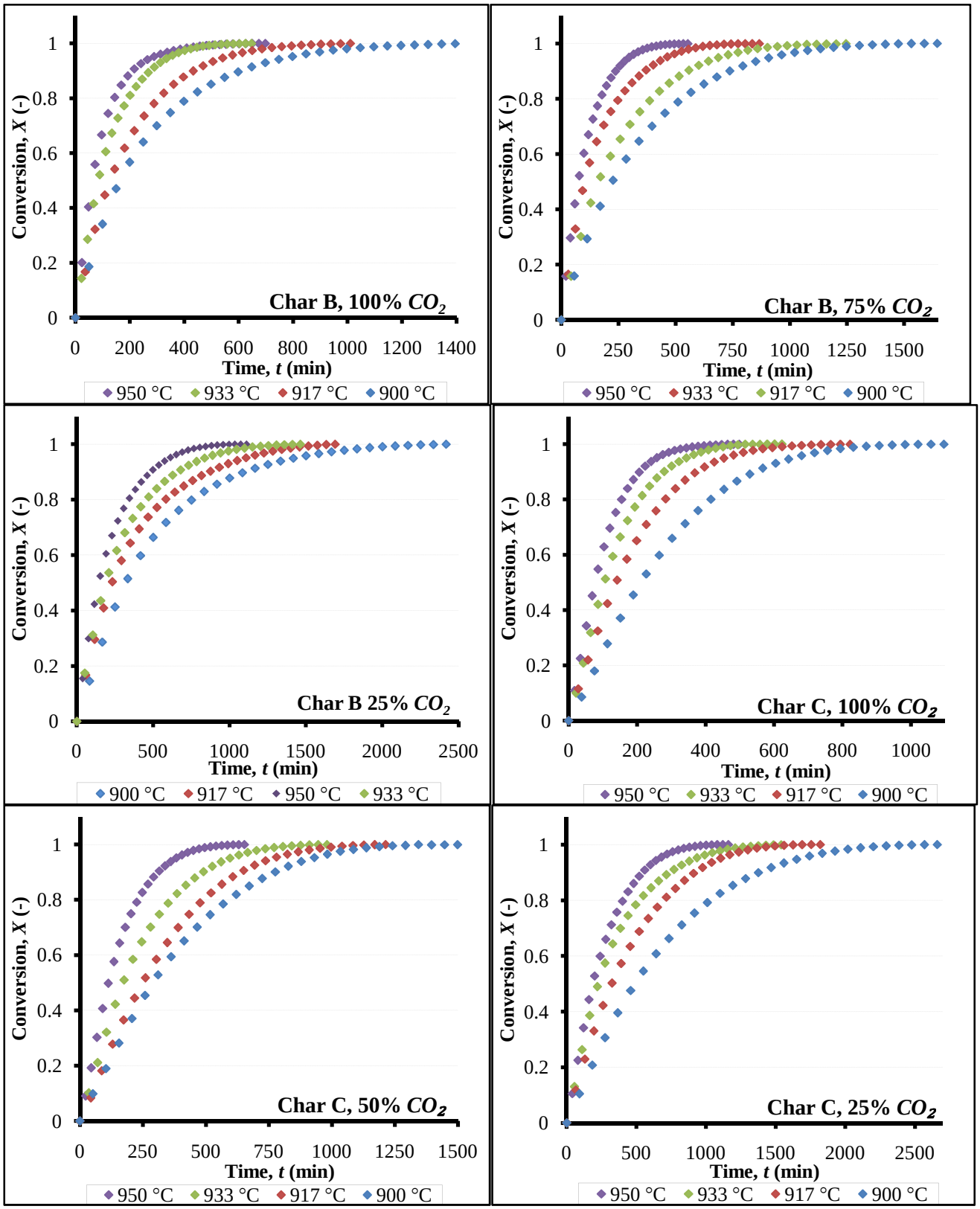

Figure B-4: Effect of temperature on the CO_2 reactivity of chars B and C, 0.875 *bar*.

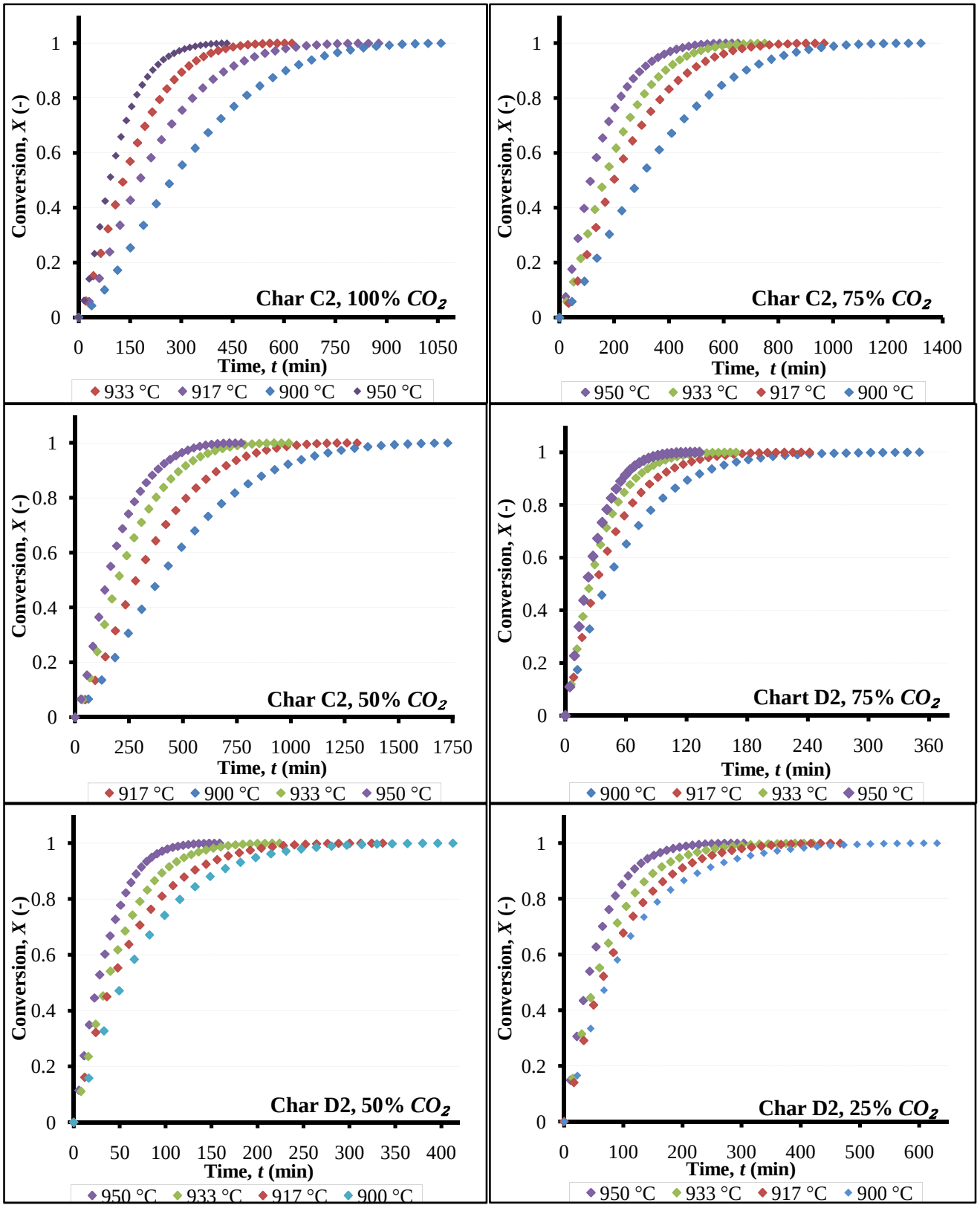

Figure B-5: Effect of temperature on the CO_2 reactivity of chars C2 and D2, 0.875 *bar*.

B-4 Effect of CO_2 Concentration in the Reaction Gas on Char Reactivity

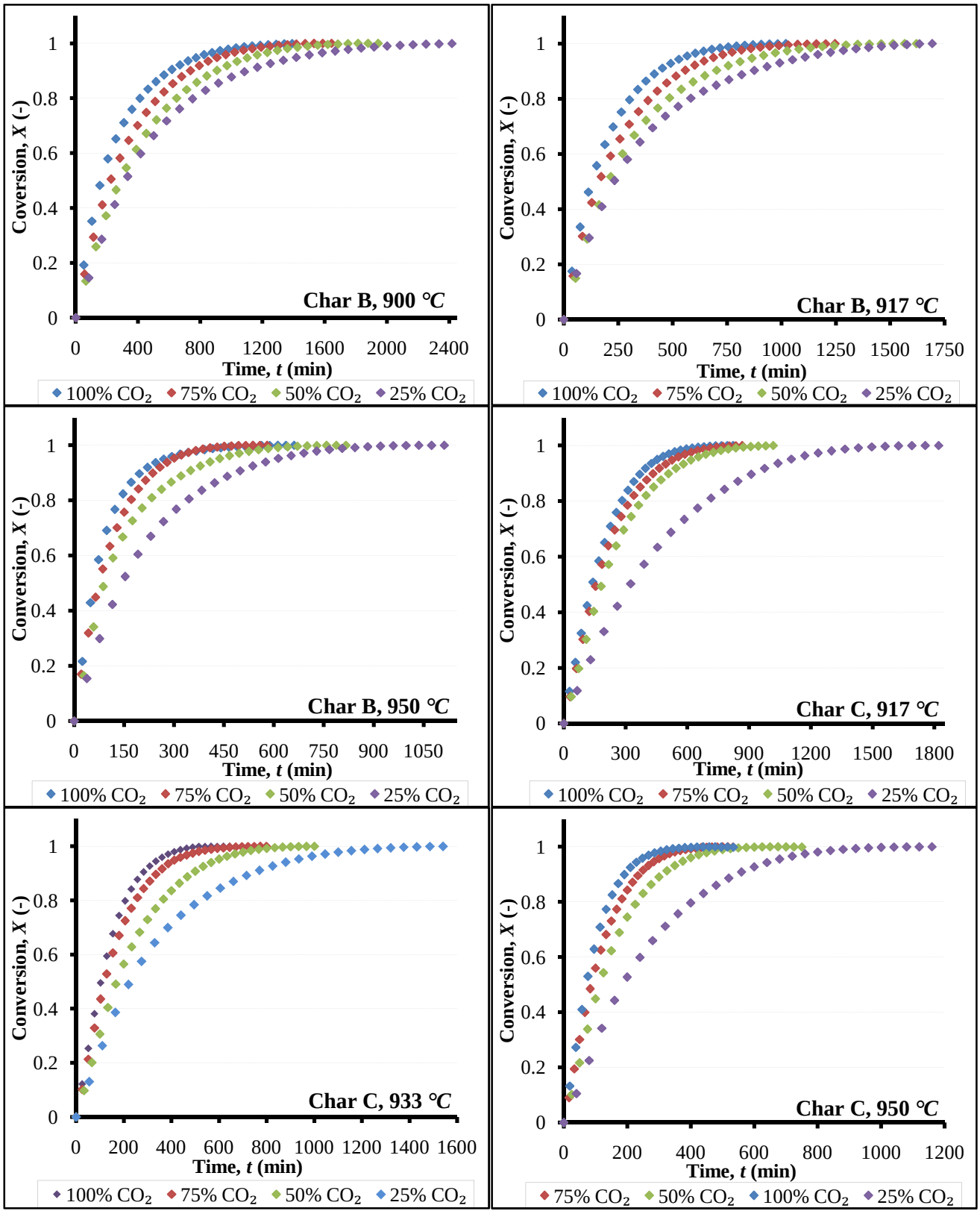

Figure B-6: Effect of CO_2 concentration on the reactivity of chars B and C, 0.875 *bar*.

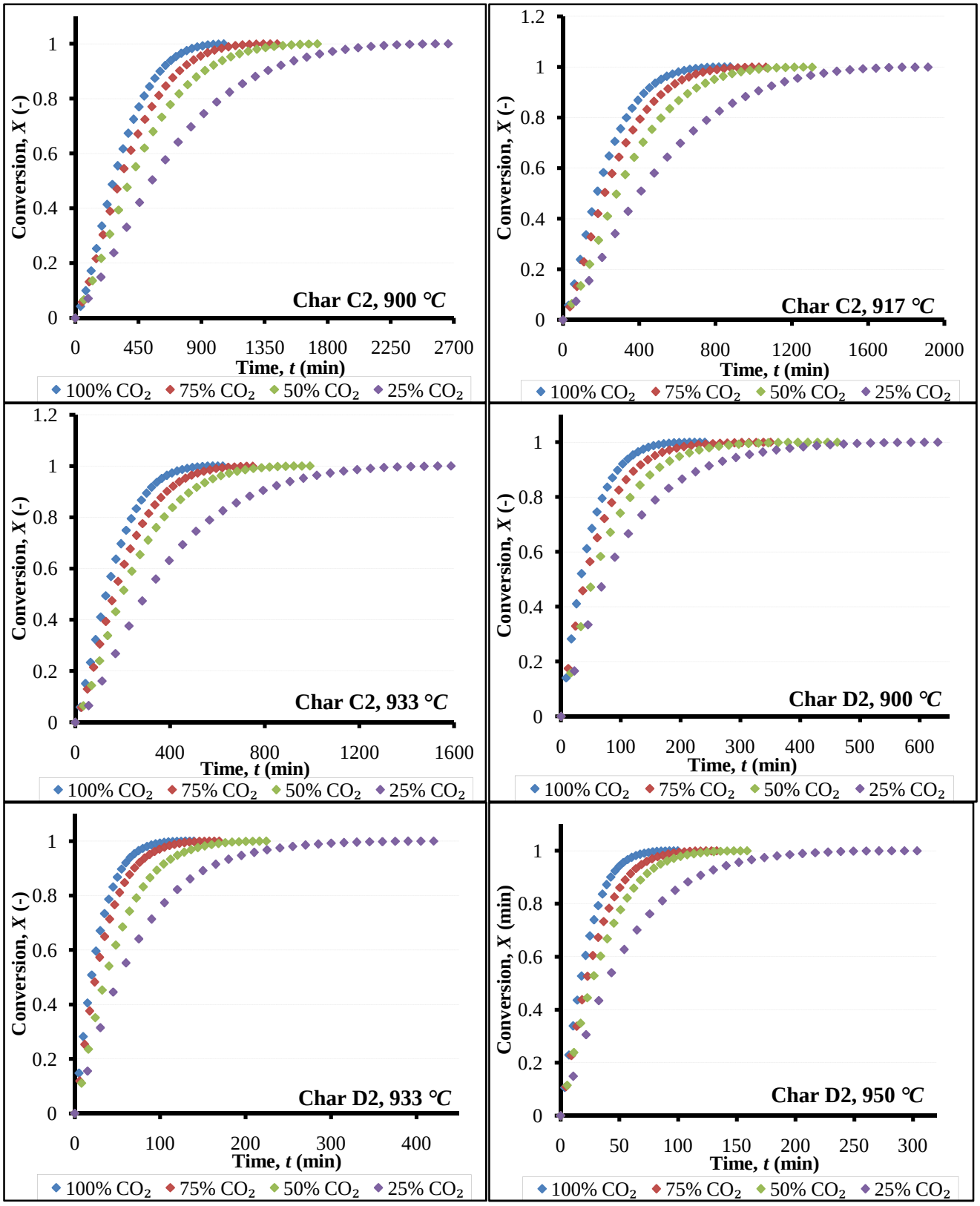

Figure B-7: Effect of CO_2 concentration on the reactivity of chars C2 and D2, 0.875 *bar*.

B-5 Comparison of CO_2 Reactivity of the Four Chars

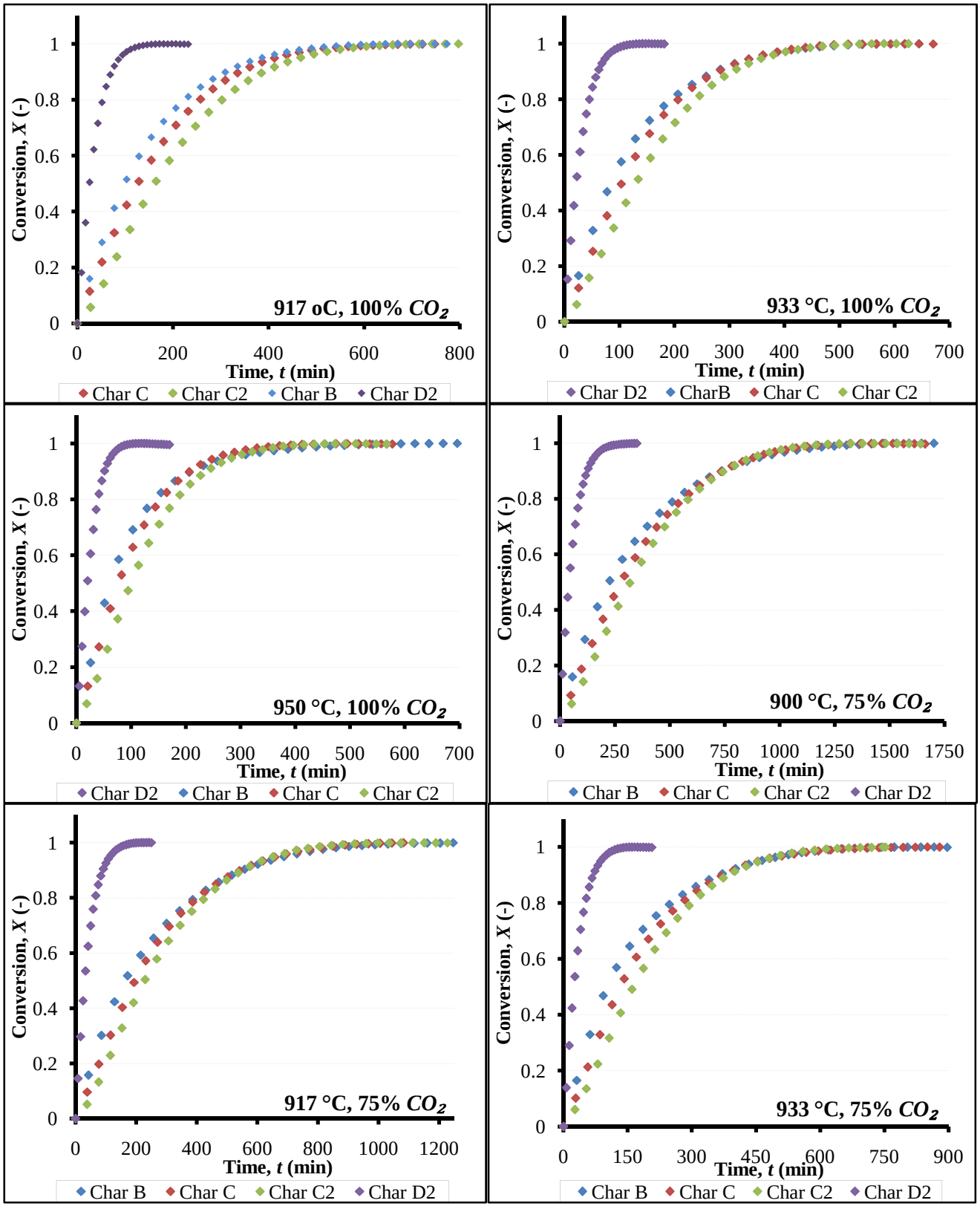

Figure B-8: Comparison of the CO_2 reactivity of chars at 100 and 75% CO_2 concentration, 0.875 *bar*.

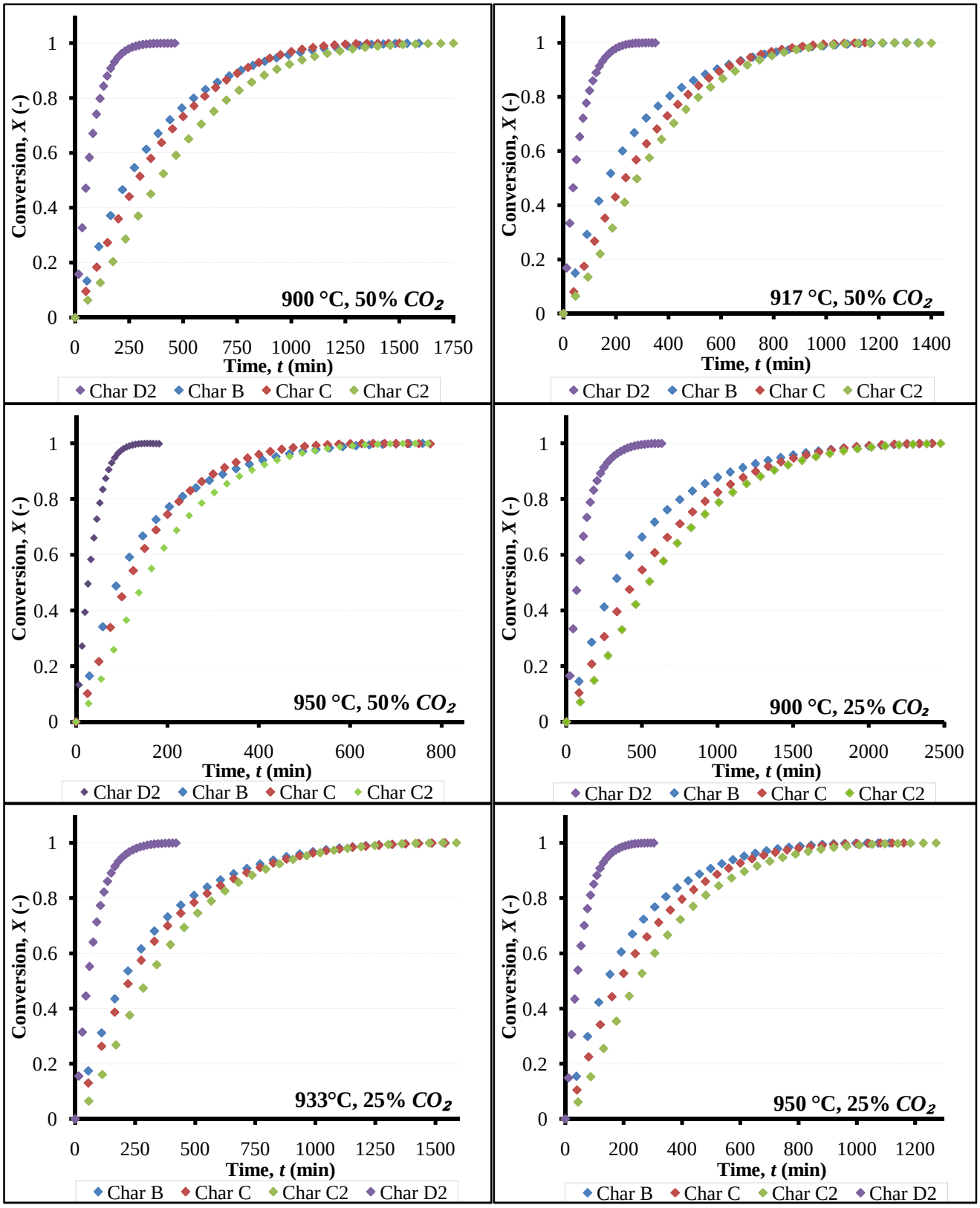

Figure B-9: Comparison of the CO_2 reactivity of chars at 50 and 25% CO_2 concentration, 0.875 *bar*.

APPENDIX C

Evaluation of Kinetic Parameters and Gasification Modelling

C-1 Summary of Structural Parameter, Time Factor and Initial Reactivity of the Chars

Table C-1: Summary of the structural parameter, time factor and initial reactivity for char C, 0.875 *bar*.

Char C						
Temp. (℃)	y_{CO_2} (*mol. %*)	$t_{0.5}$ (*min*)	$t_{0.9}$ (*min*)	$R \cdot 10^{-3}$ (min^{-1})	$t_f \cdot 10^{-3}$ (min^{-1})	ψ (-)
900 ℃	25%	489.05	1379.7	1.02	1.05	1.6500
917 ℃		322.87	920.50	1.55	1.56	1.6389
933 ℃		226.13	737.43	2.21	2.18	1.1829
950 ℃		186.08	544.00	2.69	2.73	1.5553
900 ℃	50%	289.27	773.87	1.73	1.79	1.9181
917 ℃		249.07	637.02	2.01	2.11	2.1413
933 ℃		170.80	487.05	2.93	3.01	1.4762
950 ℃		113.00	310.12	4.43	4.69	1.7483
900 ℃	75%	229.78	608.77	2.18	2.27	1.9451
917 ℃		157.02	435.15	3.19	3.37	1.6877
933 ℃		120.58	339.62	4.15	4.35	1.6422
950 ℃		86.433	237.20	5.80	6.04	1.7835
900 ℃	100%	211.20	543.13	2.37	2.49	2.1216
917 ℃		126.28	339.37	3.96	4.13	1.8508
933 ℃		104.25	278.52	4.80	5.14	1.8274
950 ℃		76.983	207.07	6.50	6.91	1.8255

Table C-2: Summary of the structural parameter, time factor and initial reactivity for char C2, 0.875 *bar*.

Char C2						
Temp. (℃)	y_{CO_2} *(mol. %)*	$t_{0.5}$ *(min)*	$t_{0.9}$ *(min)*	$R \cdot 10^{-3}$ (min^{-1})	$t_f \cdot 10^{-3}$ (min^{-1})	ψ *(-)*
900 ℃	25%	545.65	1362.07	0.92	0.99	2.3040
917 ℃		401.20	1005.68	1.25	1.33	2.3005
933 ℃		300.08	781.03	1.67	1.82	2.0101
950 ℃		247.97	620.60	2.02	2.19	2.2519
900 ℃	50%	388.72	918.52	1.29	1.38	2.7982
917 ℃		281.40	663.42	1.78	1.90	2.8881
933 ℃		198.67	485.90	2.52	2.70	2.5192
950 ℃		148.62	379.07	3.37	3.68	2.1373
900 ℃	75%	290.90	679.28	1.72	1.81	3.0163
917 ℃		198.42	478.63	2.52	2.69	2.6895
933 ℃		163.48	385.98	3.06	3.27	2.8335
950 ℃		113.33	296.83	4.41	4.80	1.9614
900 ℃	100%	271.38	605.47	1.84	1.98	3.2980
917 ℃		161.77	390.38	3.09	3.29	2.6703
933 ℃		130.62	305.62	3.83	4.04	2.9251
950 ℃		90.650	215.15	5.52	5.97	2.7396

Table C-3: Summary of the structural parameter, time factor and initial reactivity for char D2, 0.875 *bar*.

Char D2						
Temp. (℃)	y_{CO_2} ***(mol. %)***	$t_{0.5}$ ***(min)***	$t_{0.9}$ ***(min)***	$R \cdot 10^{-3}$ ***(min^{-1})***	$t_f \cdot 10^{-3}$ ***(min^{-1})***	ψ ***(-)***
900 ℃	25%	72.817	232.47	6.87	6.90	1.2117
917 ℃		62.783	191.10	7.96	8.02	1.3815
933 ℃		52.250	155.62	9.57	9.77	1.4348
950 ℃		39.017	115.58	12.8	13.1	1.4437
900 ℃	50%	53.350	159.43	9.37	9.55	1.4414
917 ℃		41.533	130.28	12.0	12.0	1.2854
933 ℃		36.133	98.217	13.8	14.5	1.7935
950 ℃		26.317	70.217	19.0	19.6	1.9396
900 ℃	75%	40.733	123.70	12.3	12.4	1.3633
917 ℃		30.450	90.033	16.4	16.9	1.4376
933 ℃		24.350	69.633	20.5	21.4	1.5567
950 ℃		21.450	56.717	23.3	24.5	1.9311
900 ℃	100%	32.633	95.183	15.3	15.8	1.4939
917 ℃		25.433	71.433	19.7	20.4	1.6372
933 ℃		19.500	55.417	25.6	26.2	1.6033
950 ℃		18.382	46.683	27.2	31.6	2.1335

C-2 Dimensionless Plots for Chars C, C2 and D2.

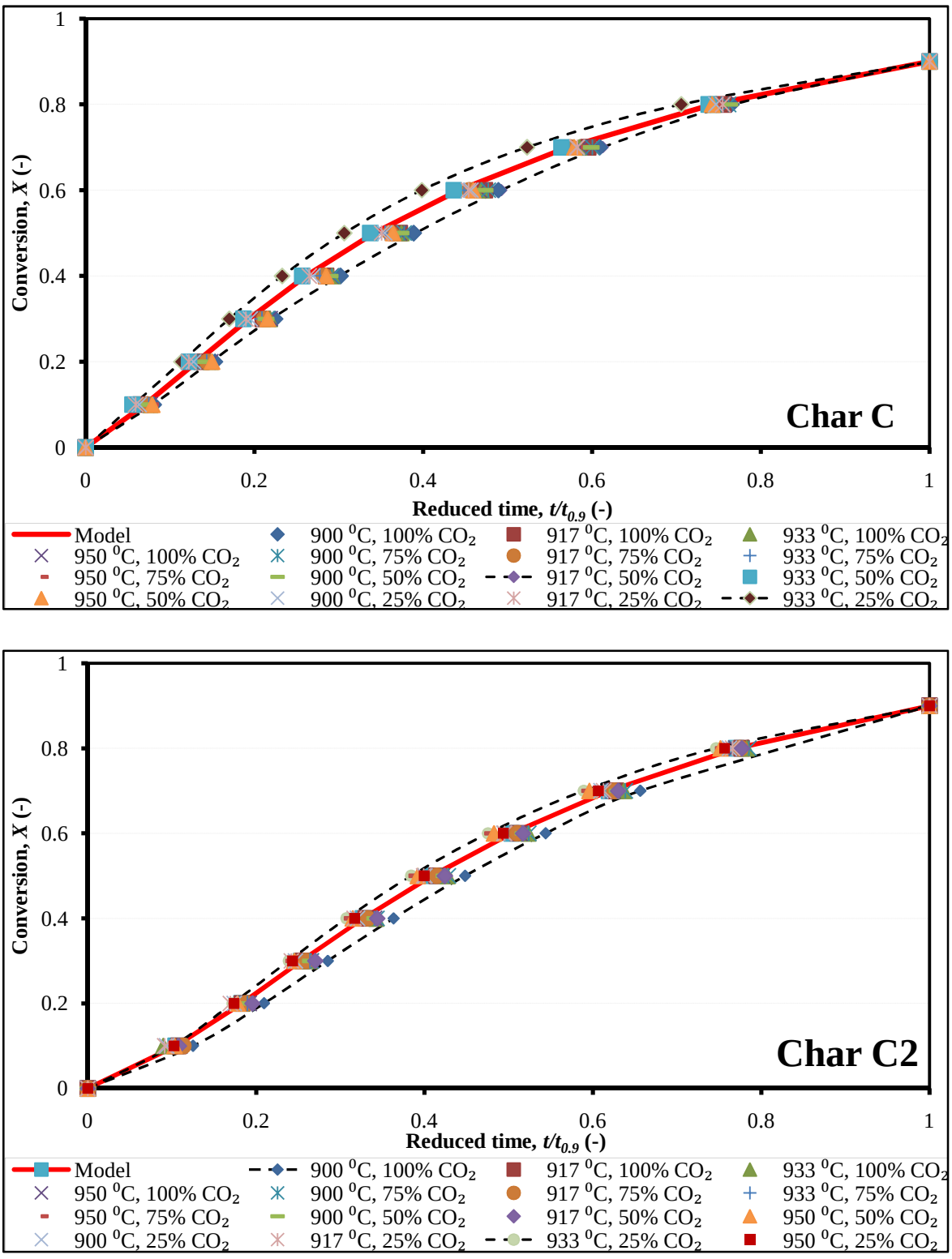

Figure C-1: Dimensionless plots of conversion versus reduced time for chars C and C2.

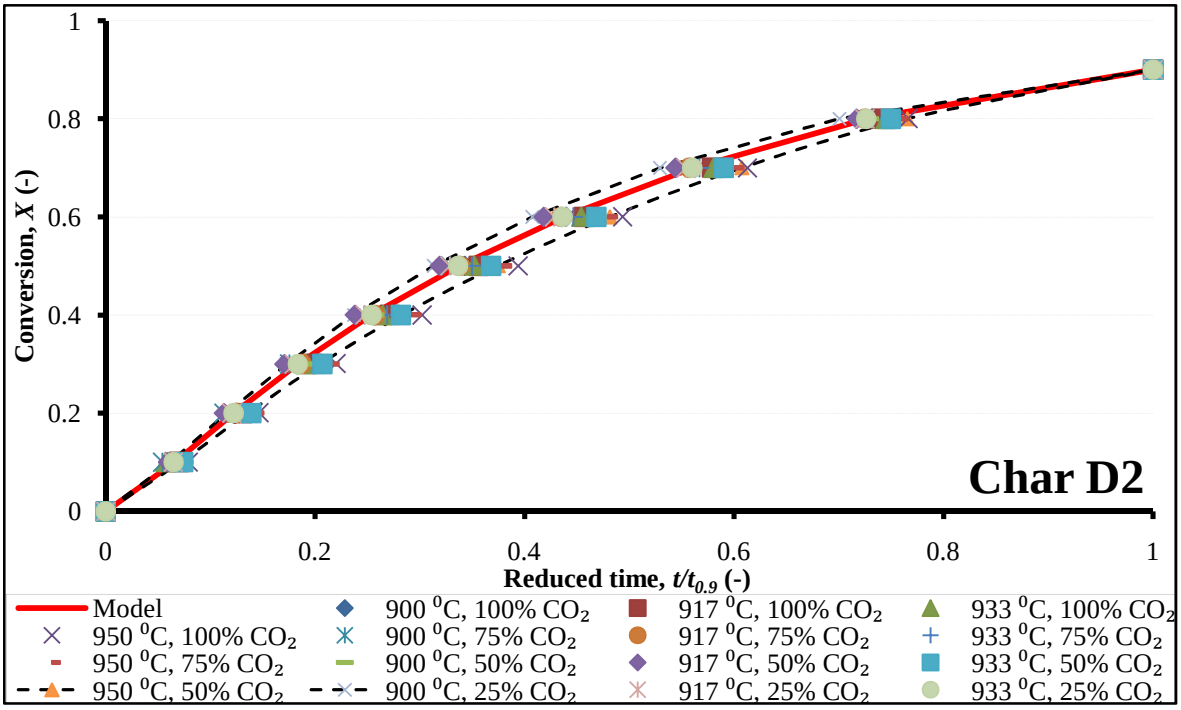

Figure C-2: Dimensionless plot of conversion versus reduced time for char D2.

C-3 Comparison of Experimental and Model Gasification Results for Chars C, C2 and D2

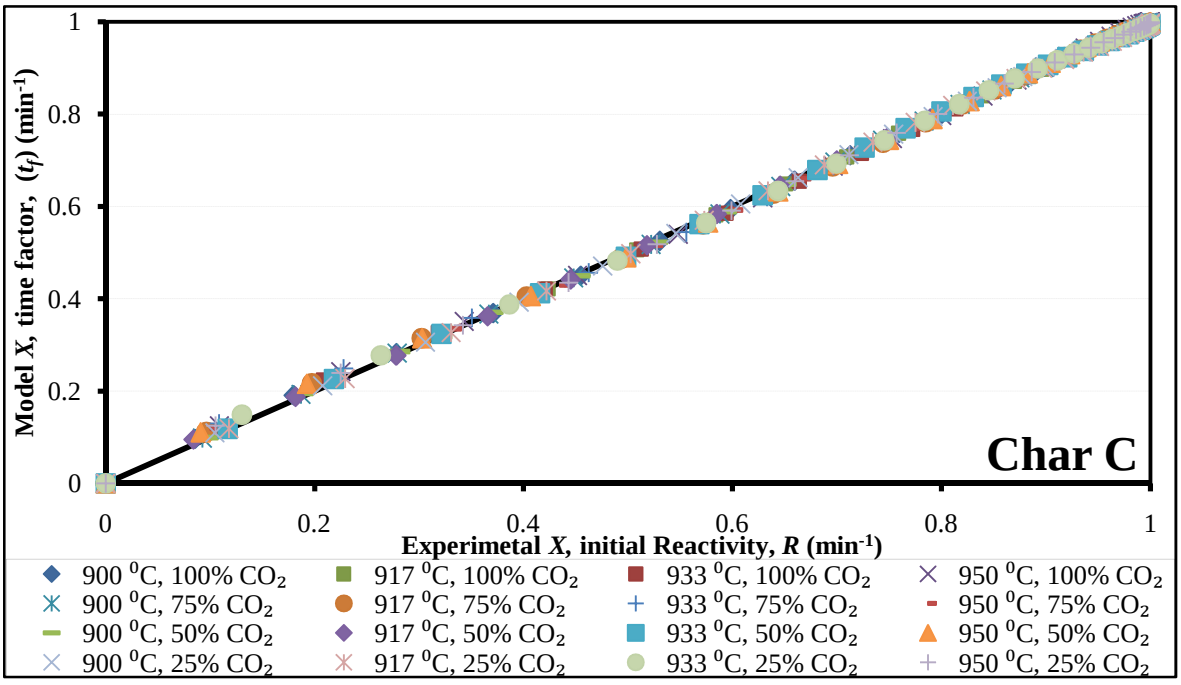

Figure C-3: Comparison between the experimental and model gasification results of char C.

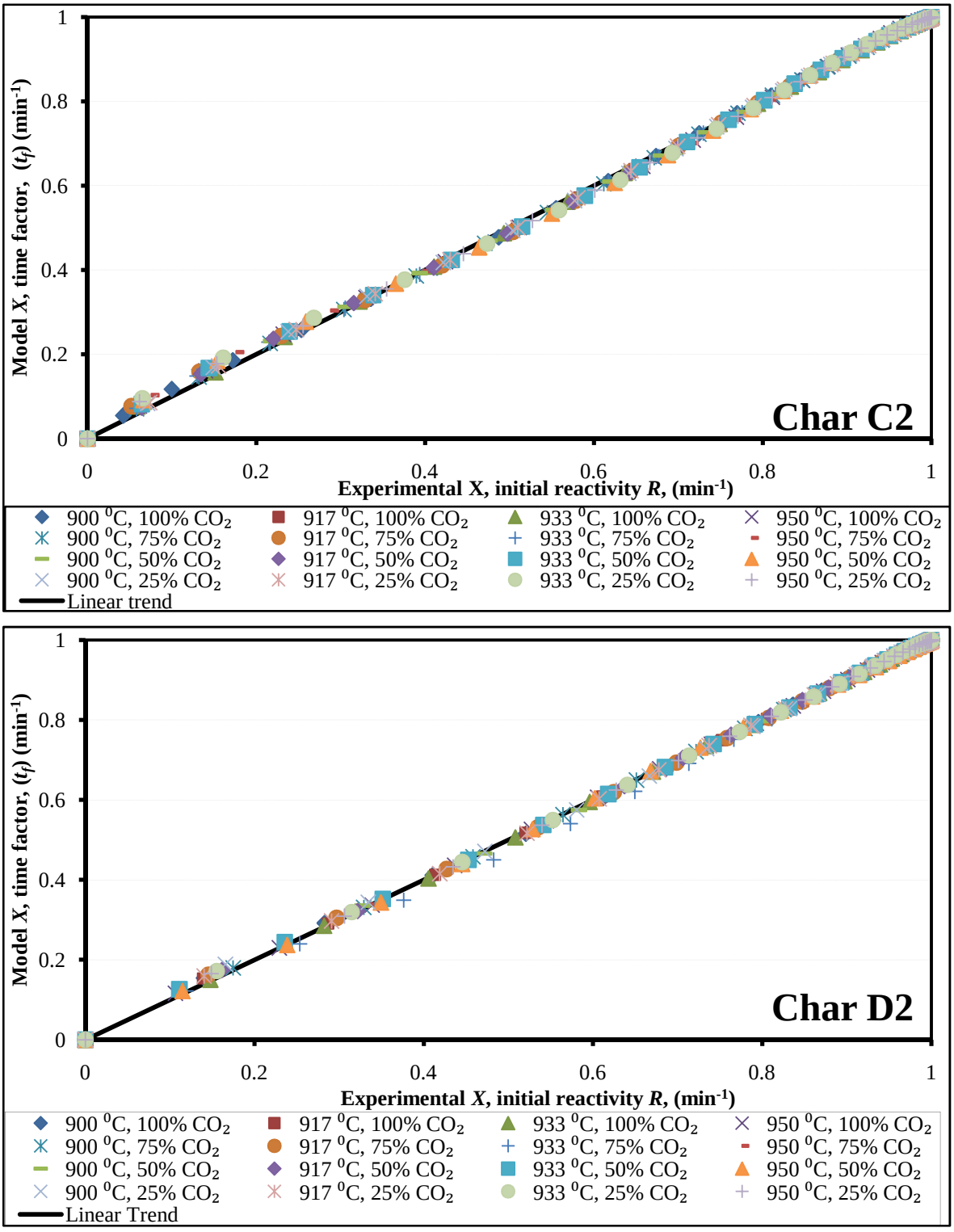

Figure C-4: Comparison between the experimental and the model gasification results of chars C2 and D2.

APPENDIX D

Model Validation: Random Pore Model (RPM)

D-1 RPM Fitting to the Experimental Data of Chars B, C, C2 and D2.

In the following figures the solid lines represent the model predicted conversions, while the points are the experimental conversions.

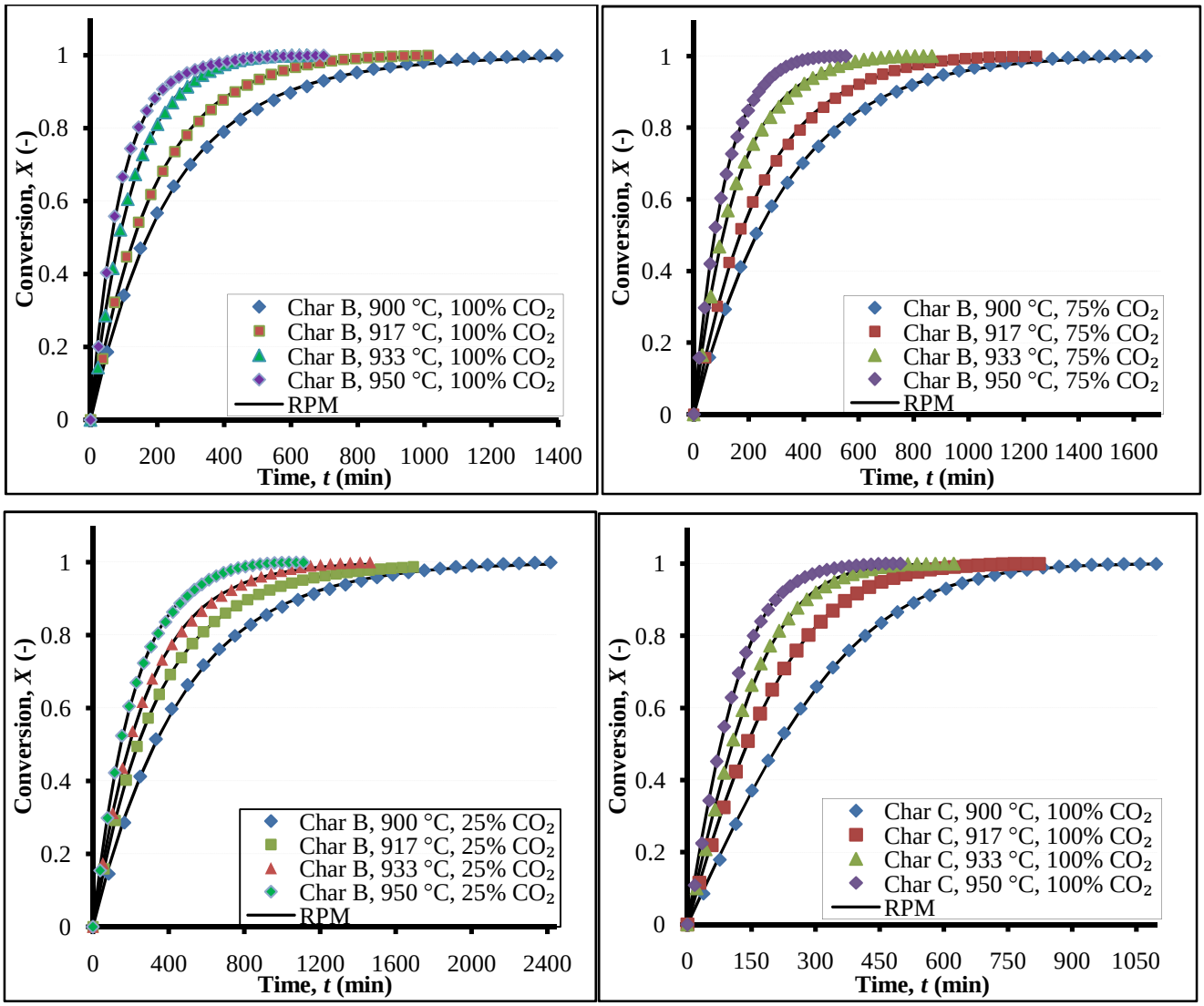

Figure D-1: RPM fitting of the experimental results of chars B and C at 0.875 *bar*.

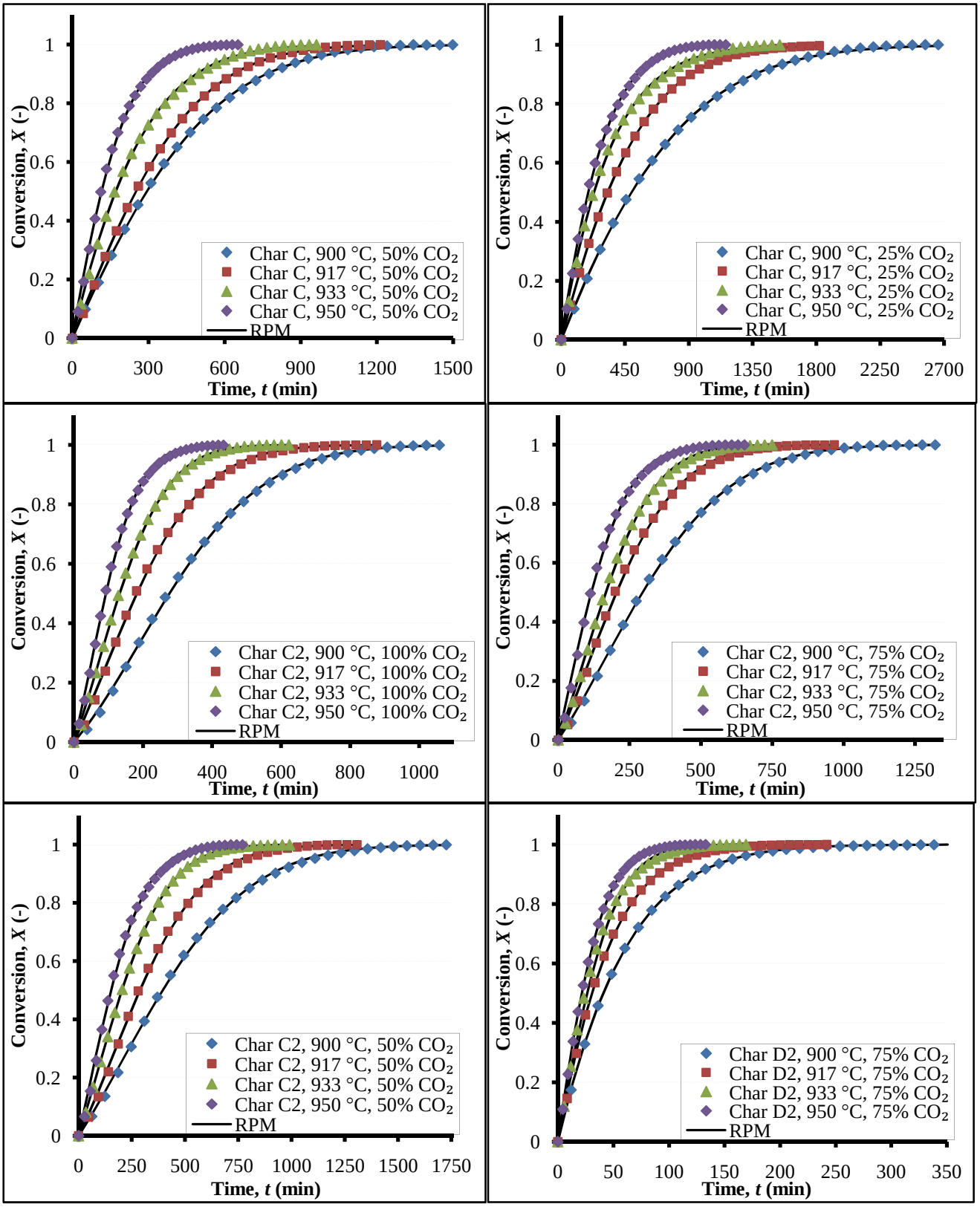

Figure D-2: RPM fitting of the experimental results of chars C, C2 and D2 at 0.875 *bar*.

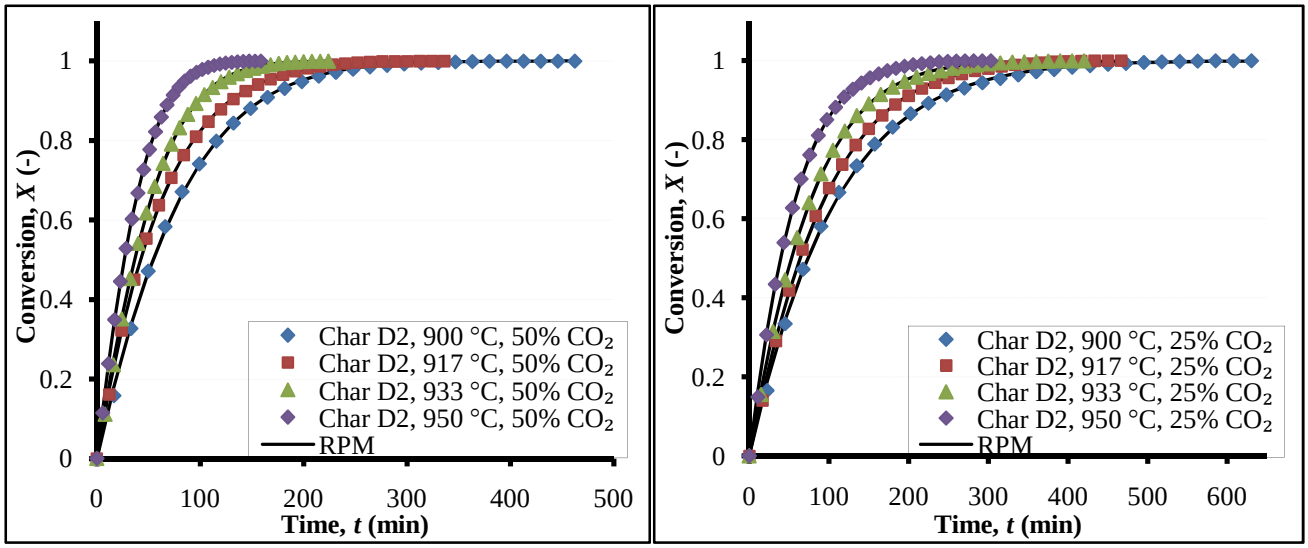

Figure D-3: RPM fitting of the experimental results of char D2 at 0.875 *bar*.

D-2 RPM Fitting of Char Conversion Rate to Experimental Results for the Chars

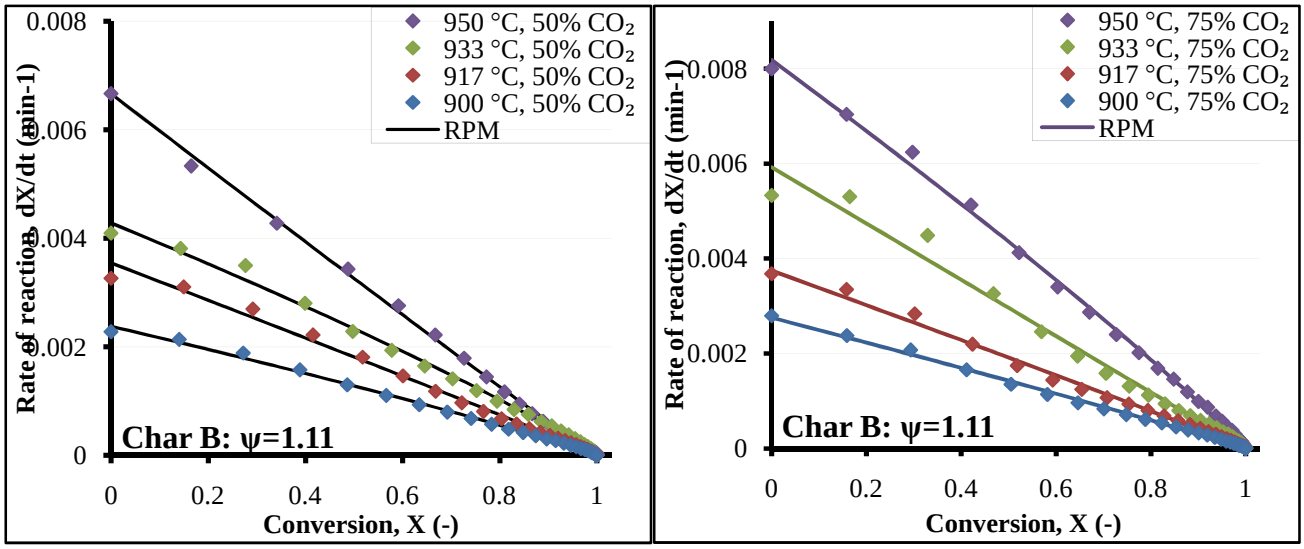

Figure D-4: RPM fitting of the char conversion rates for char B at 25% and 50% CO_2 concentration and different temperatures.

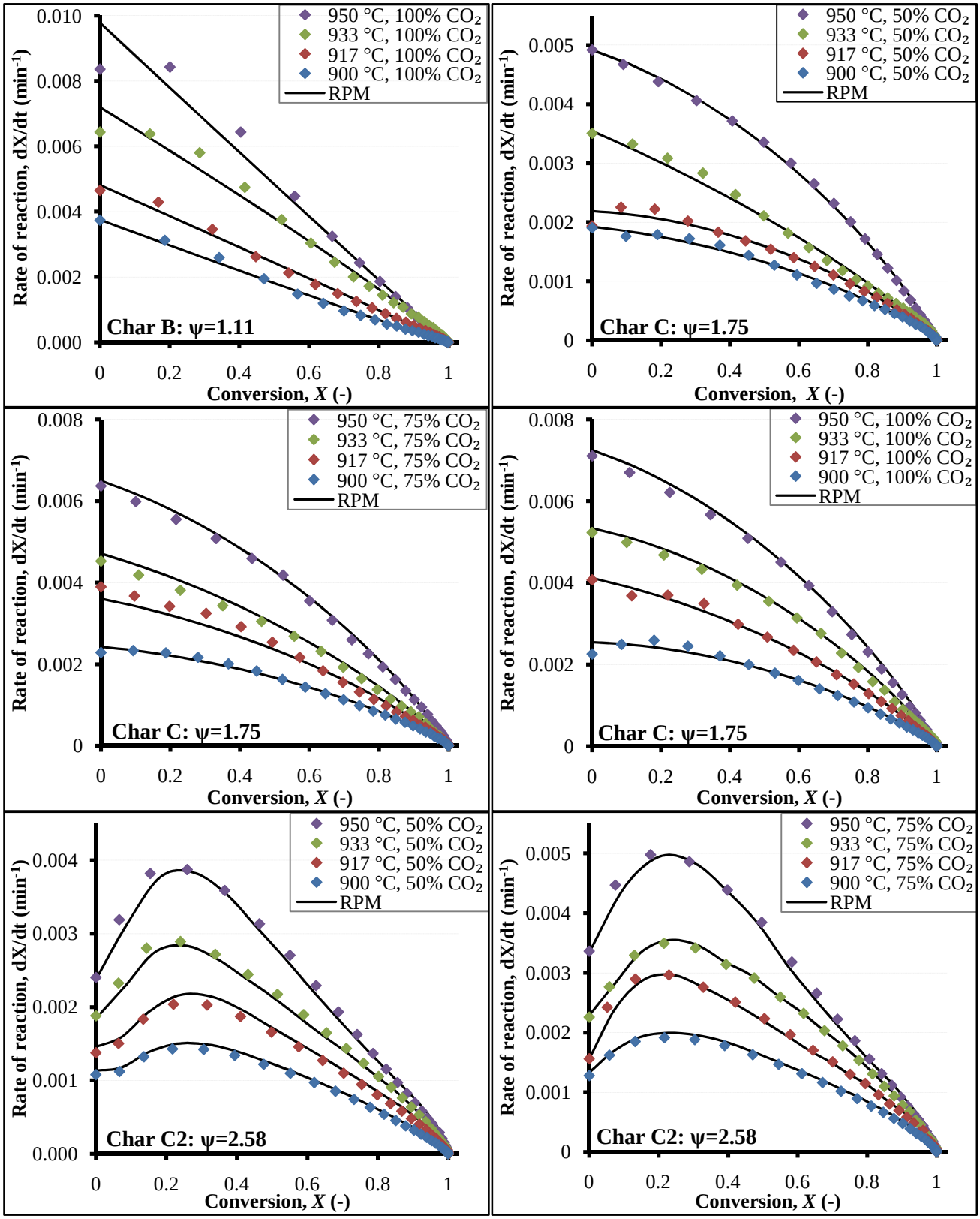

Figure D-5: RPM fitting of the char conversion rates for chars B, C, C2 at different experimental conditions, 0875 *bar*.

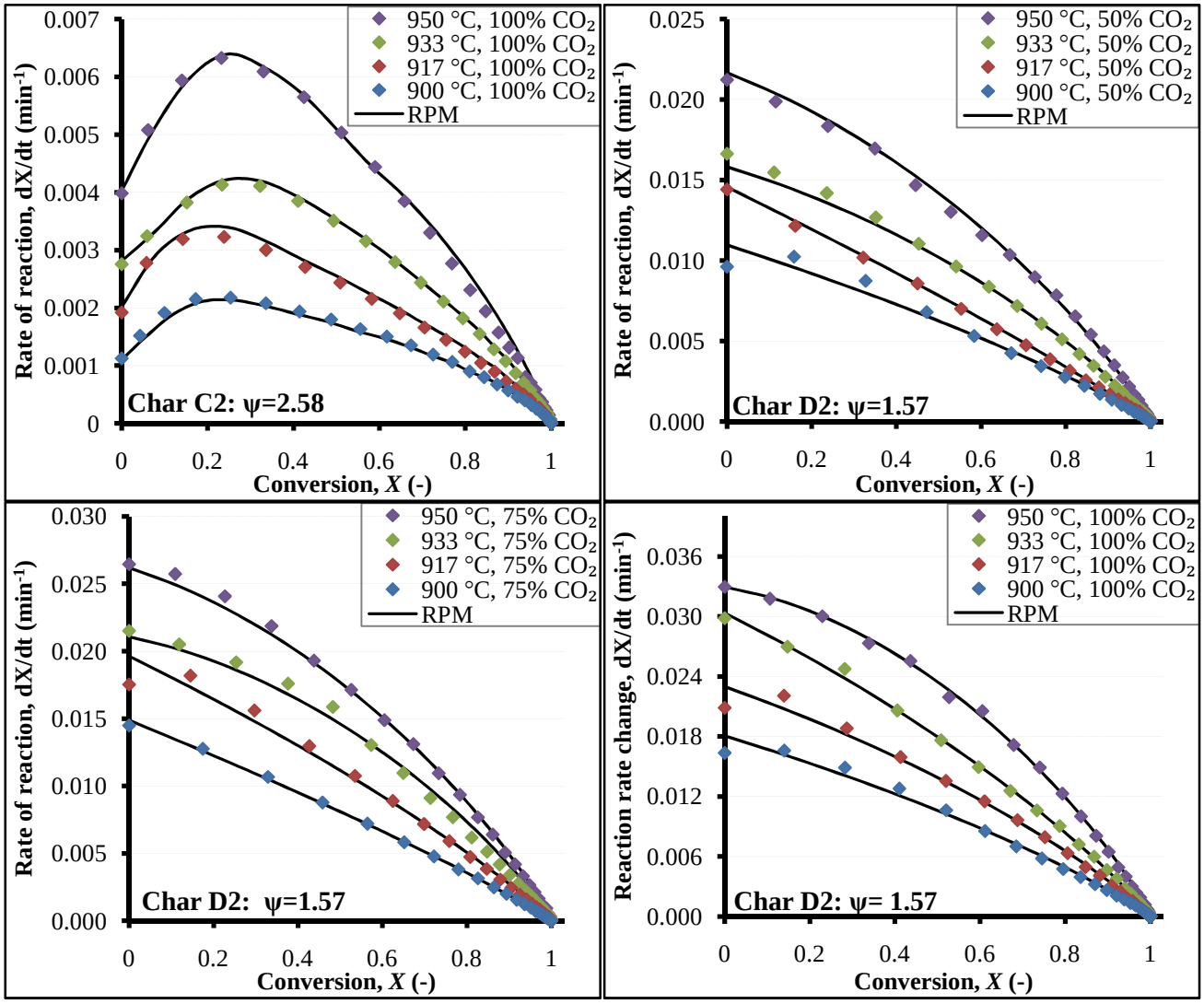

Figure D-6: RPM fitting of the char conversion rates for chars C and D2 at different experimental conditions, 0.875 *bar*.